Lateral Mobility of Proteins Adsorbed on or Embedded in Polyelectrolyte Multilayers

ARTICLE *in* LANGMUIR · SEPTEMBER 2001

Impact Factor: 4.46 · DOI: 10.1021/la0104469

5 AUTHORS, INCLUDING:

Csilla Gergely
Université de Montpellier
148 PUBLICATIONS **1,876** CITATIONS
SEE PROFILE

Bernard Tinland
French National Centre for Scientific Research
47 PUBLICATIONS **1,387** CITATIONS
SEE PROFILE

Lateral Mobility of Proteins Adsorbed on or Embedded in Polyelectrolyte Multilayers

L. Szyk,[†,‡] P. Schaaf,*[,§] C. Gergely,[†,§,||] J. C. Voegel,[†] and B. Tinland[§]

INSERM Unité 424, (UFR "Odontologie"), Université Louis Pasteur, 11 rue Humann, 67085 Strasbourg, Cedex, France, Institut Charles Sadron (CNRS−ULP), 6 rue Boussingault, 67083 Strasbourg, Cedex, France

Received March 26, 2001. In Final Form: June 18, 2001

We present the first results relative to the diffusion process of proteins (human serum albumin) adsorbed on or embedded in poly(sodium 4-styrenesulfonate)/poly(allylamine hydrochloride) polyelectrolyte multilayer films by using fluorescence recovery after photobleaching. At least two populations of adsorbed proteins exist on the top or within the multilayer architectures. One population, which typically represents 50−70% of the adsorbed proteins, corresponds to proteins that are able to diffuse laterally along the surface or in the multilayers, whereas the others diffuse more slowly or seem almost immobile over the experimental time scale. This constitutes a key result for the practical applications of the polyelectrolyte multilayers as targeted biomaterial coatings. Surprisingly, the diffusion coefficients of the mobile proteins that are embedded in the multilayers are comparable with the diffusion coefficients of the mobile proteins adsorbed on top of the multilayers. The diffusion coefficients, which are 1 order of magnitude smaller than on rigid substrates such as silica or poly(methyl methacrylate), are of the order of 10^{-10} and 10^{-11} cm^2/s.

Introduction

In the field of biomaterials the most striking advances in the past decade have been achieved in the design of new bioactive materials.[1] These materials exhibit bioactivity properties mainly through biological recognition. Such recognition can either result from the incorporation of active molecules in the bulk of the materials or by their immobilization on the material surfaces. In this latter case, the molecules are usually covalently bound or immobilized by simple adsorption on the surfaces. A new, promising method based on the alternate adsorption of polycations and polyanions on charged surfaces has been developed recently.[2,3] The buildup of polyelectrolyte multilayers offers great advantages over the covalent coupling and adsorption methods; one can easily adsorb and incorporate proteins[4] or other particles[5] on and into the multilayer films. Moreover, proteins embedded in the films keep, at least partially, their biological activity.[6] All these properties allow the assembly of complex architectures with targeted properties.[7] One should, for example, be able to adsorb on or incorporate in such films proteins such as fibronectin, fibrinogen, and vibronectin promoting the adhesion of cells. Cell adhesion is, however, strongly influenced by the degree of mobility of the ligands along the surface.[8] The extent of cell spreading, for example, depends on both the overall amount of ligands immobilized on the surface and their ability to cluster into spatial microdomains.

The first systematic studies of adsorption of proteins on solid surfaces covered by polyelectrolyte multilayers have been undertaken recently.[9,10] Proteins usually adsorb on both positively and negatively charged multilayers, the adsorbed amount being the highest when the protein and multilayer have opposite charges. The high protein coverages observed are incompatible with adsorption of the protein molecules at random positions without any surface diffusion. However, to the authors' knowledge, no study relative to the diffusion of proteins adsorbed on or embedded in multilayer films or even on polyelectrolyte monolayers has been reported up to now. It is the goal of this investigation to provide such information.

Fluorescence recovery after photobleaching (FRAP) constitutes a method well suited to undertake such a study.[11,12] FRAP has been used to investigate the diffusion of adsorbed proteins on various solid surfaces such as poly(methyl methacrylate) (PMMA) or glass. The diffusion coefficients usually appear to be about 10^{-9} to 10^{-10} cm^2/s as summarized in a recent review of Tilton.[13] In this study we use human serum albumin adsorbed on or inserted in poly(sodium 4-styrenesulfonate) (PSS)/poly(allylamine hydrochloride) (PAH) multilayer films at pH 7.4 as a model system. At this pH, human serum albumin is negatively charged and adsorbs more readily on PAH- than on PSS-terminating films.[9] We will thus present results relative to the diffusion of human serum albumin on both kinds

* To whom correspondence should be addressed.
† Université Louis Pasteur.
‡ Current address: Institute of Catalysis and Surface Chemistry, Polish Academy of Sciences, 30−239 Cracow, ul. Niezapominajek, Poland.
§ Institut Charles Sadron.
|| Home laboratory: Institute of Biophysics, Biological Research Centre of the Hungarian Academy of Science, Szeged H-6701, Hungary.

(1) Hubbell, J. A. *Curr. Opin. Biotechnol.* **1999**, *10*, 123.
(2) Decher, G.; Hong, J.-D. *Makromol. Chem. Macromol. Symp.* **1991**, *46*, 321.
(3) Decher, G. *Science* **1997**, *277*, 1232.
(4) Onda, M.; Lvov, Y.; Ariga, K.; Kunitake, T. *Jpn. J. Appl. Phys.* **1997**, *36*, L1608.
(5) Serizawa, T.; Takeshita, H.; Akashi, M. *Langmuir* **1998**, *14*, 4088.
(6) Caruso, F.; Niikura, K.; Furlong, D. N.; Okahata, Y. *Langmuir* **1997**, *13*, 3427.
(7) Hammond, P. T. *Curr. Opin. Colloid Interface Sci.* **2000**, *4*, 430.
(8) Kusumi, A.; Suzuki, K.; Koyasako, K. *Curr. Opin. Cell Biol.* **1999**, *11*, 582.
(9) Ladam, G.; Gergely, C.; Senger, B.; Decher, G.; Voegel, J.-C.; Schaaf, P.; Cuisinier, F. J. G. *Biomacromolecules* **2000**, *1*, 674.
(10) Ladam, G.; Schaaf, P.; Cuisinier, F. J. G.; Decher, G.; Voegel, J.-C. *Langmuir* **2001**, *17*, 878.
(11) Davoust, J., Devaux, P. F.; Leger, L. *EMBO J.* **1982**, *10*, 1233.
(12) Axelrod, D.; Koppel, D. E.; Schlessinger, J.; Elson, E.; Webb, W. W. *Biophys. J.* **1976**, *16*, 1055.
(13) Tilton, R. D. In *Biopolymers at Interfaces*; M. Malmsten, Ed.; Marcel Dekker: New York, 1998; Chapter 11.

10.1021/la0104469 CCC: $20.00
Published on Web 09/12/2001

of terminating multilayers and also report results relative to human serum albumin embedded in such architectures.

Materials and Methods

Human serum albumin-fluorescein isothiocyanate (HSA) and trishydroxyaminomethane (Tris) were purchased from Sigma Chemical Co. Anionic poly(sodium4-styrenesulfonate) (MW = 70000) (PSS), cationic poly(allylamine hydrochloride) (M_n = 50000−65000) (PAH), and cationic poly(ethyleneimine) (MW = 750000) (PEI) were purchased from Aldrich. Sodium chloride was purchased from Fluka. All the products of commercial origin were used without further purification. Ultrapure water from a Millipore system was used for the preparation of the buffers and solutions and for the different cleaning steps. The resistivity of the water was approximately 18 MΩ. The concentration of Tris-HCl buffer solution was 5×10^{-4} M, and the pH was adjusted to 7.4 by addition of some droplets of concentrated HCl. NaCl was added to the solution to adjust the ionic strength to 150 mM.

Multilayers Surface Preparation. The multilayers were built on rectangular silica microslide capillaries (internal dimensions: 0.2 × 2.0 mm²; length, 100 mm) purchased from Wale Apparatus Co. (Hellertown, PA). The capillaries were first cleaned with a detergent solution (RBS, Roth-Sochiel Sarl, France) in an ultrasonic cleaner. They were then well rinsed with distilled water before being soaked in concentrated nitric acid for approximately 1 h. Each capillary was then thoroughly rinsed with ultrapure water and stored in water until used. The storage never exceeded 4 days. The multilayers were built as follows.

First, the capillary was rinsed with Tris-HCl buffer. The first PEI layer was then adsorbed from a PEI solution (c_{PEI} = 5 mg/mL in 1 M NaCl). The capillary was filled with the polyelectrolyte solution with the use of a syringe, and the solution was kept in contact with the capillary for 20 min. The capillary was then rinsed with 10 mL of Tris-HCl for 5 min before the PSS solution (c_{PSS} = 0.5 mg/mL in 1 M NaCl) was injected and kept in the capillary for 30 min. After rinsing with Tris-HCl, the PAH solution (c_{PAH} = 0.5 mg/mL in 1 M NaCl) was injected into the capillary and, as previously, kept in contact for 30 min with the surface before being rinsed with Tris-HCl again. The same procedure was repeated by alternating PSS and PAH adsorption until the final polyelectrolyte architecture was attained. Two polyelectrolyte multilayer films were chosen: a PAH-terminating film, PEI(PSS/PAH)$_3$, and a PSS-terminating film, PEI(PSS/PAH)$_2$PSS.

Adsorption of HSA. HSA, at a concentration of 0.5 mg/mL in 0.15 M NaCl Tris-HCl, was adsorbed on the outer layer of the polyelectrolyte film, directly on bare silica or on a PMMA surface. The chosen HSA bulk concentration was far in the adsorption plateau domain of albumin for each of the three surfaces.[9] In the PMMA a homemade cell with PMMA walls was used. The adsorption time was always 2 h, and after this time, the capillary or the cell in the PMMA was rinsed with 10 mL Tris-HCl buffer at a flow rate of 0.01 mL/s, allowing the removal of all the loosely bound albumin molecules from the capillary. The surface diffusion coefficient of adsorbed albumin was then measured.

For the measurement of the diffusion coefficient of HSA embedded in the multilayer film six further polyelectrolyte layers were deposited on the HSA ending structure from polyelectrolyte solutions prepared in 0.15 M NaCl, 5×10^{-4} M Tris-HCl buffer, to avoid albumin denaturation. This led to PEI−(PSS/PAH)$_3$−HSA−(PAH/PSS)$_3$ and PEI−(PSS/PAH)$_2$−PSS−HSA−(PSS/PAH)$_3$ architectures.

Fluorescence Recovery after Photobleaching. The diffusion coefficient of fluorescein-labeled HSA was measured by a fringe pattern fluorescence bleaching technique similar to the one described by Davoust et al.[11] The most important difference, as it was described by van Blaaderen et al.,[14] is that the same beam was used for reading and bleaching. This experimental setup is easier to align and ensures a better stability of the positions of the reading fringes with respect to the bleached fringe pattern. It is schematically depicted in Figure 1. The light beam of an etalon-stabilized monomode Ar laser (1 W at a wavelength

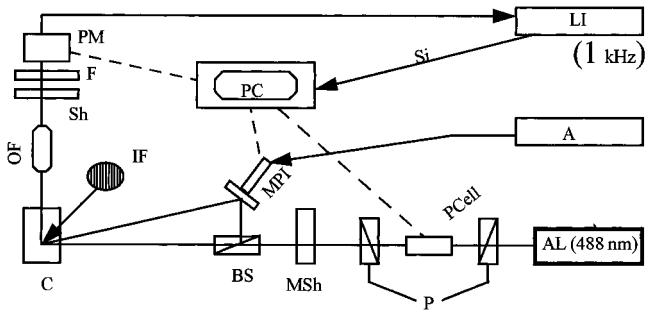

Figure 1. Schematic representation of the FRAP apparatus. Abbreviations: PM, photomultiplier; F, filter; Sh, shutter; MSh, manual shutter; OF, optic fiber; C, capillary; BS, beam splitter; IF, interference fringes; PC, personal computer; Si , signal; LI, lock-in; A, amplifier; AL, argon laser; P, polarizers; Pcell, Pockels cell; PMI, piezo-mirror.

λ = 488 nm) is split and the two beams crossed in the capillary cell providing illumination in a deep sinusoidal interference fringe pattern. The fringe spacing $i = 2\pi/q$ set by the crossing angle ϕ, $q = (4\pi/\lambda)\sin(\phi/2)$, ranges from 1 to 60 μm, defining the diffusion distance range. Fluorescence bleaching of the labeled species in the illuminated fringes is obtained by producing a 1-s full-intensity bleach pulse by means of a Pockels cell between nearly crossed polarizers. After bleaching, the pattern is monitored by the same fringe pattern, produced by the two crossed beams at a very low intensity. The fluorescent signal is picked up by an optical fiber, and the scattered light is filtered out. To protect the photomultiplier during the bleach pulse the high-intensity signal is blocked by a shutter. The fringes are spatially modulated by a sinusoidally vibrating mirror (≈1 kHz). The mirror is piezoelectrically driven in a direction normal to its surface with an amplitude that is of the same order as the fringe spacing i. The fluorescence emission of the bleached sample is now modulated as the bleached pattern, and the moving illuminating fringes fall in and out of phase; the change of the fluorescence signal is obtained with lock-in detection. The switching in the setup is controlled by a microcomputer that also collects the data. The use of the same fringe pattern for the bleaching and the reading ensures that they are both characterized by the same spatial wavelength, which leads, for this method, to the best signal-to-noise ratio.

Davoust et al.[11] showed that the component of the fundamental frequency of the fluorescence intensity detected in the locking-in amplifier varies with time as:

$$I_f(t) = I_1 \exp(-t/\tau) + I_0 \qquad (1)$$

where I_0 (respectively, I_1) corresponds to the intensity caused by the immobile (respectively, mobile) proteins. The diffusion coefficient D of the labeled molecules is related to τ according to $\tau = 1/Dq^2$. Measurements performed for different values of q were performed to check if τ varies linearly with q^{-2}, which is a signature of a diffusive process. In our experiments we investigated q vectors ranging from 6000 cm^{-1} to 4500 cm^{-1}, which corresponds to a fringe spacing i ranging from 10 μm to 14 μm. To protect the sample from photobleaching during experiments (typical duration, 20 min) we used a shutter, so that the sample was only illuminated by the light for 10 s every 30 s. From the exponential decay function (*1*) we could also determine the mobile protein fraction f on the surface which is given by:

$$f = \frac{I_1}{I_0 + I_1} \qquad (2)$$

Determination of the Surface Coverage and the Thickness of Adsorbed HSA Layers. The surface concentration was determined with the FRAP equipment working as a fluorometer. In this case the fluorescent intensity was measured immediately after injection of the albumin solution into the capillary. Then, after 2 h of adsorption, the cell was rinsed and the fluorescent intensity was measured again. The concentration Γ_{alb} of albumin

(14) van Blaaderen, A.; Peetermans, J.; Maret, G.; Dhont, J. K. G. *J. Chem. Phys.* **1992**, *96*, 4591.

adsorbed on the surface is then given by:

$$\Gamma_{alb} = \frac{F_S \cdot C_b \cdot V}{F_b \cdot 2S} \quad (3)$$

where F_S and F_b are the fluorescent intensities [mV] on the surface and in the bulk, respectively, C_b is the bulk concentration of albumin [mg/cm^3], V the volume of solution in the capillary [cm^3], and S is the surface area [cm^2] of the capillary illuminated by the laser beam. The factor 2 comes from the fact that the fluorescent intensity originates from both sides of the rectangular capillary.

We used also optical waveguide lightmode spectroscopy (OWLS) to characterize the structure of the polyelectrolyte multilayer films and to determine the amounts of HSA adsorbed on top of them. OWLS is an optical technique in which a light beam is coupled into a waveguide through a coupling grating. From the coupling angles one gets information about the thickness and the refractive index of the film deposited on top of the $Si_{0.8}Ti_{0.2}O_2$ waveguide. We have used a homemade apparatus similar to that described in refs 15 and 16 as well as similar analysis methods to extract the structural parameters from the rough optical data.

Results and Discussion

Structural Properties of the Adsorbed Films. OWLS allowed us to follow the buildup process of the polyelectrolyte architectures, further albumin adsorption and the subsequent polyelectrolyte depositions. (PSS/PAH)$_n$ multilayers are known to consist of stratified structures in which the polyanions and polycations of individual layers interdigitate the nearest neighboring layers intimately.[17,18] Because of this interdigitation such films can, as far as OWLS experiments are concerned, be considered as homogeneous and isotropic monolayers.[19] Typical evolutions of the adsorbed amounts found for the PEI−(PSS/PAH)$_3$−HSA−(PAH/PSS)$_3$ and PEI−(PSS/PAH)$_2$−PSS−HSA−(PSS/PAH)$_2$PSS films during their buildup are given in Figure 2. Before protein adsorption, the multilayer thickness (data not shown) and the amount of polyelectrolyte deposited increased linearly with the number of (PSS/PAH) bilayers as it is usually observed.[3] One can point out that, unlike other optical techniques, OWLS allows accurate measurement of the properties of the first deposited layers even without surface drying. We found that each (PSS/PAH) bilayer contributed to increase the optical thickness by approximately 6 nm and the adsorbed amount by about 0.7 μg/cm^2 consistent with previous results.[20] We observed further that the amounts of polyanion and polycation constituting a bilayer are not exactly equal but that, in our case, the amount of deposited PSS is slightly larger than that of PAH on the same bilayer as reported previously.[18,21] The amounts of HSA adsorbed on both PSS- and PAH-terminating multilayer films and determined by FRAP are consistent within about 30% with those found by OWLS. Differences of this order are typically found in protein adsorption experiments. These adsorbed amounts and the albumin layer thickness are given in Table 1. The albumin molecules in aqueous solution are usually represented as prolate ellipsoids of revolution with dimensions equal to 12 × 2.7 × 2.7 nm[3,22] or 14.1 × 4.1 × 4.1 nm[3,23] and a molecular weight of 69000. Assuming that the molecules are adsorbed in "end on" configurations, one gets a coverage of 14% (respectively, 31%) on PSS- and 37% (respectively, 86%) on PAH-terminating films taking the adsorbed amount determined by fluorescence into account. On both films HSA molecules should thus adopt "end on" and "side on" configurations. It is expected, however, that on PSS-terminating films most molecules are adsorbed in the "side on" configuration, whereas on PAH-terminating films HSA molecules form a dense monolayer of proteins adsorbed mainly in "end on" configurations. This is confirmed by the thickness of the adsorbed layers determined by OWLS and which are equal to 5 and 13 nm on PSS- and PAH-terminating films, respectively. One observes also in the insets of Figure 2 that, during the rinsing step of the experimental cell by pure buffer after HSA adsorption, no protein is desorbed even at the initial rinsing stages (the beginning of rinsing is indicated by a mark), indicating that the HSA molecules can be considered as irreversibly bound on the polyelectrolyte multilayers during the fluorescence experiments.

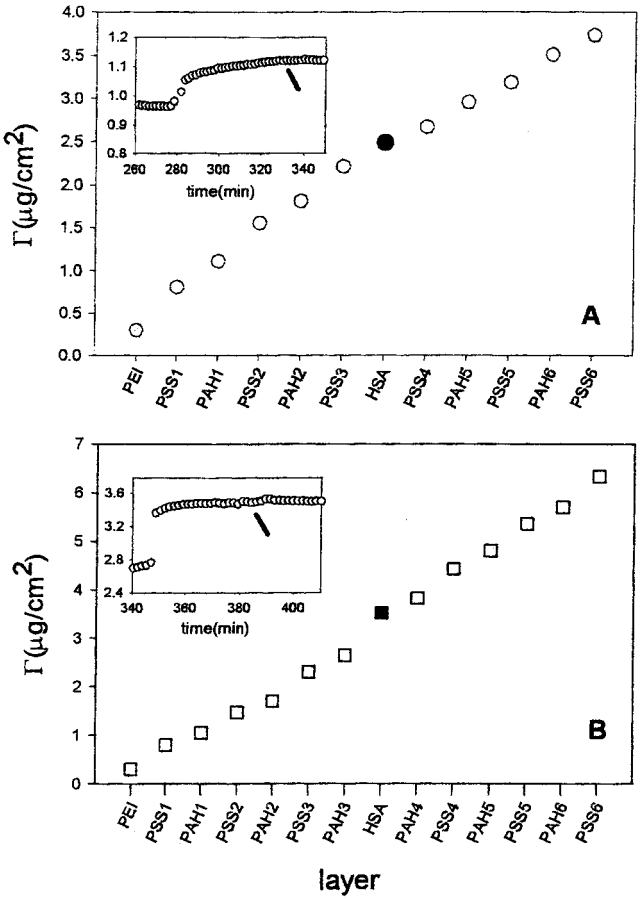

Figure 2. Typical evolution of the adsorbed albumin amounts (Γ) for the PEI−(PSS/PAH)$_2$−PSS−HSA−(PSS/PAH)$_2$PSS (A) and PEI−(PSS/PAH)$_3$−HSA−(PAH/PSS)$_3$ (B) films during their buildup determined from OWLS data. Open symbols correspond to polyelectrolyte addition; full symbols, HSA adsorption. The insets show the adsorption kinetics of HSA. The marks indicate the start of the pure buffer injection step; no protein desorption is observed. The abscissas correspond to the different steps of the buildup process: PEI, PEI; PSS1, PEI/PSS; PAH1, PEI−(PSS/PAH)$_1$; PSS2, PEI−(PSS/PAH)$_1$−PSS; PAH2, PEI−(PSS/PAH)$_2$.

(15) Ramsden J. J.; Prenosil, J. E. *J. Phys. Chem.* **1994**, *98*, 5376.
(16) Ball, V.; Ramsden, J. J. *J. Phys. Chem.* **1997**, *101*, 5465.
(17) Schmitt, J.; Grünewald, T.; Decher, G.; Pershan, P. S.; Kjaer, K.; Lösche, M. *Macromolecules* **1993**, *26*, 7058.
(18) Lösche, M.; Schmitt, J.; Decher, G.; Bouwman, W. G.; Kjaere, K. *Macromolecules* **1998**, *31*, 8893.
(19) Picart, C.; Ladam, G.; Senger, B.; Voegel, J. C.; Schaaf, P.; Cuisinier, F. J. G.; Gergely, C. *J. Chem. Phys.* **2001**, *115*, 1086.
(20) Ladam, G.; Schaad, P.; Voegel, J.-C.; Schaaf, P.; Decher, G.; Cuisinier, F. J. G. *Langmuir* **2000**, *16*, 1249.
(21) Ramsden, J. J.; Lvov, Y. M.; Decher, G. *Thin Solid Films* **1995**, *254*, 246.
(22) Haynes, C. A.; Norde, W. *Colloids Surfaces B: Biointerfaces* **1994**, *2*, 517.
(23) Peters, T. *Adv. Protein Chem.* **1985**, *37*, 161.

Table 1. Surface Diffusion Coefficients of Embedded or Adsorbed HSA Amounts on Various Surfaces[a]

multilayer architecture	concentration of HSA in the solution c_{HSA} (mg/cm^3)	diffusion coefficient D (cm^2/s)	mobile fraction f[b]	surface concentration Γ (μg/cm^2)		thickness of HSA layer d_A (nm) OWLS
				FRAP	OWLS	
silica−HSA	0.5	$1.09 \pm 0.06 \times 10^{-9}$	0.4	0.015		
PMMA−HSA	0.5	$3.21 \pm 0.21 \times 10^{-9}$	0.15	0.30		
−PAH−HSA	0.5	$1.02 \pm 0.07 \times 10^{-10}$	0.7	0.59	0.88	13
−PSS−HSA	0.5	$6.62 \pm 0.71 \times 10^{-11}$	0.4−0.6	0.23	0.24	5
−PAH−HSA−PAH−	0.5	$1.33 \pm 0.63 \times 10^{-10}$	0.3			
−PSS−HSA−PSS−	0.5	$1.12 \pm 0.74 \times 10^{-10}$	0.5			

[a] Abbreviations: −PAH−HSA and −PSS−HSA correspond, respectively, to the PEI(PSS/PAH)$_3$−HSA and to the PEI(PSS/PAH)$_2$PSS−HSA architectures, whereas −PSS−HSA−PSS− and −PAH−HSA−PAH− correspond, respectively, to the PEI(PSS/PAH)$_2$PSS−HSA−(PSS/PAH)$_3$ and to the PEI(PSS/PAH)$_3$−HSA−(PAH/PSS)$_3$ architectures. [b] On PSS terminating films and when HSA is inserted between PSS layers f represents the fraction of rapidly diffusing molecules.

The fact that on PAH-terminating films HSA forms only a monolayer for the protein concentrations used seems at first sight to be in contradiction with the thick HSA film extending up to 4 times the largest size of the molecule as found by scanning angle reflectometry.[9,10] The experiments of Ladam et al.[9,10], however, were performed with HSA purified by the Cohn method.[24] This method is known for not removing the fatty acids bound to the albumin molecules, whereas our experiments were conducted with essentially fatty acid-free albumin. The differences in the adsorption property of HSA purified by the two methods, however, do not diminish the importance of the present study in which HSA was only chosen as a test protein to determine whether proteins can diffuse on multilayer films and to get an estimate of their diffusion coefficients.

We determined also by fluorescence the amount of HSA adsorbed on a silica and on a PMMA surface. The amount adsorbed on silica (0.015 μg/cm^2) is very small compared with that found on both polyelectrolyte multilayer films. It corresponds to a coverage of the order 2−4% and indicates that the affinity of HSA for silica is much smaller than for both negatively and positively charged polyelectrolyte surfaces. It was expected that the amount of HSA adsorbed on a silica surface is much smaller than on a PAH-ending multilayer. The smaller affinity of HSA for silica than for a PSS-ending films can have several causes. Both surfaces are negatively charged at pH 7.4. However, PSS is slightly hydrophobic through its phenyl rings, whereas silica is mainly hydrophilic. Moreover, silica constitutes a rigid substrate, whereas the polyelectrolyte chains of PSS are flexible. Interactions with underlying PAH chains eventually are also possibly caused by the interdigitation of neighboring layers.[17,18] Finally, PMMA is a more hydrophobic substrate than silica, and one finds that the amount of HSA adsorbed on PMMA (0.3μg/cm^2) is of the same order as the amounts adsorbed on PAH (0.6μg/cm^2)- and PSS (0.23μg/cm^2)-terminating polyelectrolyte multilayer films.

Surface Diffusion of HSA Molecules on and in Multilayer Films. Figure 3 presents typical curves of the evolution with time of the fluorescence intensity relative to HSA molecules adsorbed on a PAH (Figure 3A)- and on a PSS (Figure 3B)-terminating film, after an initial sample bleaching ($t = 0$). In the HSA on PAH the intensity decreases over a time scale which is of the order of 300 s in Figure 3A before reaching a constant non-zero value. These curves were treated by the exponential function (*1*) during a time ranging from 0 to t and t was gradually increased. The fitting parameters were constant within 10% during the whole experimental time. This is illustrated by the inset of Figure 3A where $\ln[I_f(t) - I_0]$ varies linearly with time throughout the whole experiment. In the HSA adsorbed on PSS-terminating films, the fluorescence intensity decrease clearly exhibits at least two time scales. The long time scale exceeds the time during which the experiment is conducted so that the signal does not reach a constant value (Figure 3B).When such a curve was treated by the exponential function (*1*) during a period of time t and t was gradually increased, the fitting parameters were constant within 10% over times up to 1200 s for Figure 3B. The parameters then changed gradually when the fitting function (*1*) was applied over longer times. This is illustrated in the inset of Figure 3B where the linear dependence of $\ln[I_f(t) - I_0]$ with time is only observed up to 1200 s. [I_0 corresponds to the value determined by fitting $I_f(t)$ with function (*1*) over times shorter than 1200 s.] In both cases (on PAH and PSS) there thus seem to exist at least two populations of adsorbed HSA molecules: a population of "rapidly" diffusing molecules and a population of "slowly" diffusing ones. In the HSA adsorbed on PAH-terminating films molecules seem immobile at our experimental time scale. Our FRAP experimental setup allows us only to analyze the diffusion of the most rapidly diffusing proteins, responsible for the observed initial exponential decay of the fluorescence intensity; in the following text the "rapidly" diffusing population is simply called the "mobile" fraction.

The fluorescence experiments were performed at different q's, and from the fit function (*1*) we determined both the characteristic time τ appearing in the exponential and the mobile fraction f. In Figure 4 we represent typical evolutions of $1/\tau$ as a function of q^2 for HSA adsorbed on PAH- and PSS-terminating films, respectively. This evolution is fully compatible with a linear dependence of $1/\tau$ with q^2. This indicates that the time evolution of the measured fluorescence is indeed caused by a diffusion process of the proteins along the surface. The diffusion coefficient is obtained from the slope of the line. The mobile fractions f and the diffusion coefficients D relative to the HSA molecules on the different surfaces are compiled in Table 1. The mobile fraction f and the diffusion coefficient D of HSA adsorbed on silica are of the order of 40% and 1.1×10^{-9} cm^2/s, respectively, in accordance with reported values.[25] On PMMA we find $f = 15\%$ and $D = 3.2 \times 10^{-9}$ cm^2/s, respectively. This value of the mobile fraction f is smaller than the 40% reported for bovine serum albumin adsorbed on a similar surface.[26] However, our value of f on PMMA is not unexpected when compared with the

(24) Cohn, E. J.; Hughes, W.; Wear, J. H. *J. Am. Chem. Soc.* **1947**, *69*, 1753.

(25) Chan, V.; Graves, D. J.; Fortina, P.; McKenzie, S. E. *Langmuir* **1997**, *13*, 320.

(26) Tilton, R. D.; Gast, A. P.; Robutson, C. R. *Biophys. J.* **1990**, *58*, 1321.

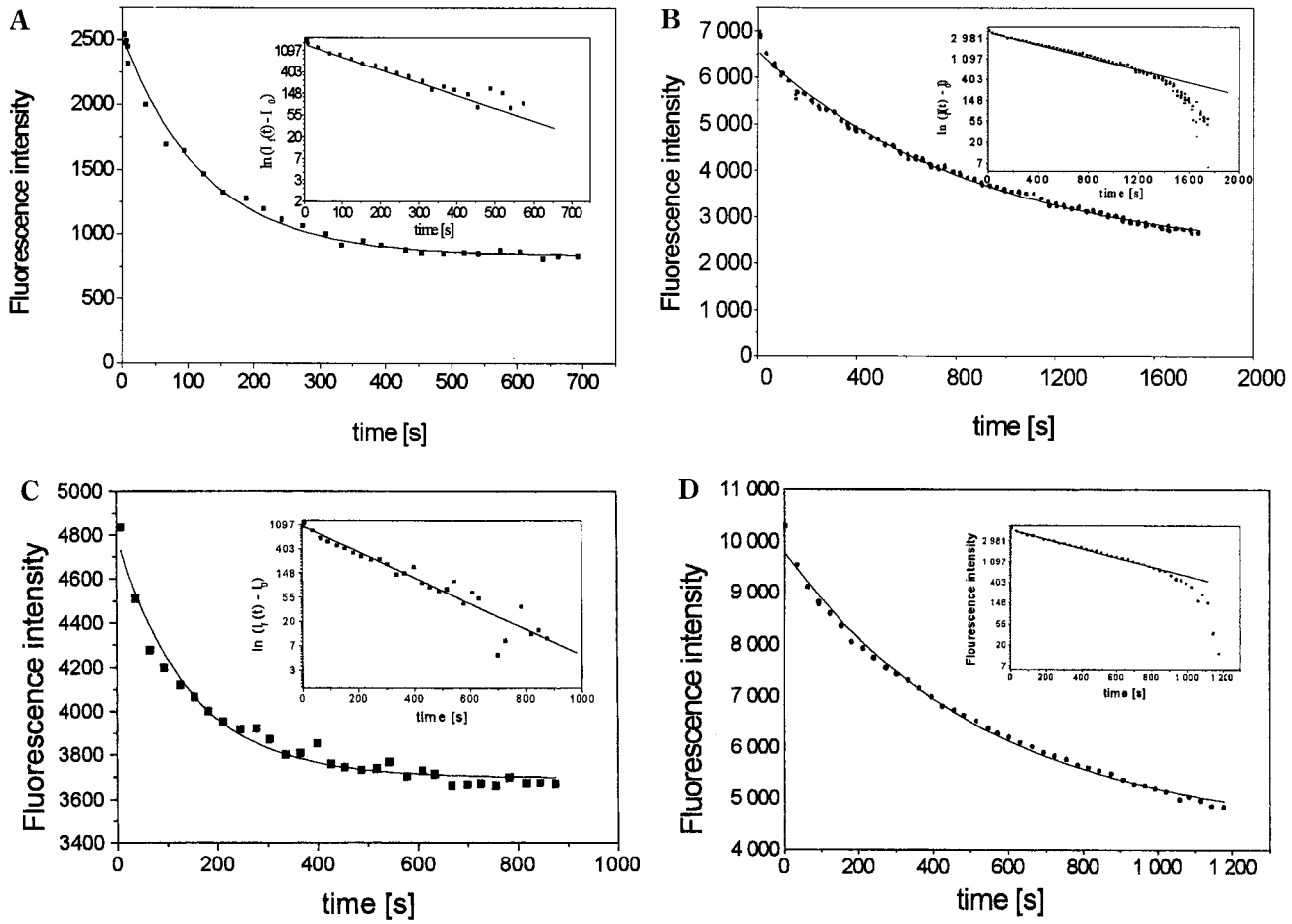

Figure 3. Evolution of the fluorescent intensity $I_f(t)$ relative to HSA adsorbed on or embedded in a multilayer film as a function of time after bleaching. The insets present the evolution of $\ln(I_f(t) - I_0)$ as a function of time for the same data. The value of I_0 corresponds to the value of the parameter I_0 determined by fitting $I_f(t)$ with the exponential function (*1*) over the time range during which the fitting parameters remained constant within 10% (see text). Points represent the experimental data; the solid lines correspond to the single-exponential fit (*1*) to the data. (A) HSA adsorbed on a PAH-terminating film; (B) HSA adsorbed on a PSS-terminating film; (C) HSA embedded between PAH layers; (D) HSA embedded between PSS layers.

relative value on a silica surface because of the partial hydrophobic nature of PMMA. On the other hand, the diffusion coefficient of HSA on PMMA is in full agreement with the value determined by Tilton et al.[26] On PAH- and PSS-terminating films, respectively, we measure values of D equal to 1.0×10^{-10} cm^2/s and 6.6×10^{-11} cm^2/s. The mobile fractions of adsorbed proteins are of the order of 70% on PAH- and between 40% and 60% on PSS-ending films. In this latter case the determined mobile fraction represents a lower estimate of f because it corresponds only to the most rapidly diffusing protein population and another more slowly diffusing one exists. The mobile fraction of adsorbed HSA molecules thus seems to be higher on the polyelectrolyte multilayers than on the "harder" investigated surfaces (silica and PMMA). On the other hand, the diffusion coefficients of HSA on the polyelectrolyte films are definitely smaller than on the "harder" surfaces, which indicates a much slower diffusion process.

All the diffusion experiments reported up to now were performed within 6 h after HSA adsorption. To check whether proteins change their diffusive properties after longer residence times, we determined also the evolution of their diffusion properties for times up to 4 days. During this time the capillaries remained filled with the pure buffer solution used during the last rinsing step. Two kinds of experiments were conducted. For one series of experiments we kept the capillaries at 4 °C overnight to avoid or to decrease eventual HSA denaturation during storage. In a second series of experiments the capillaries were kept at room temperature during the whole experimental period. No evolutions, either for the mobile fractions or for the diffusion coefficients, were observed during periods lasting more than 3 to 4 days whatever the storage conditions of the capillaries. This seems to indicate that there is no aging effect of the proteins on and in the multilayers as far as their diffusion properties are concerned.

Finally, we determined also the diffusion properties of HSA molecules embedded in polyelectrolyte multilayer films. Two kinds of architectures were investigated: PEI−$(PSS/PAH)_3$−HSA−$(PAH/PSS)_3$ and PEI−$(PSS/PAH)_2$−PSS−HSA−$(PSS/PAH)_3$. Typical curves of the evolution with time of the fluorescence intensity relative to HSA molecules embedded between PAH and PSS layers are represented in Figures 3C and 3D, respectively. The relative diffusion coefficients and mobile fractions are also presented in Table 1. One first observes that the fraction f of mobile proteins decreases significantly when HSA is embedded between PAH layers when compared with HSA adsorbed on PAH-terminating films. On the other hand, the mobile fraction f is the same, within experimental uncertainty, for the proteins embedded between PSS layers and the proteins adsorbed on PSS-terminating films. When HSA is inserted between PSS layers one observes, as for HSA adsorption on PSS-terminating films, a slight decrease of the fluorescence intensity after long adsorption times, and the exponential fit function (*1*) could

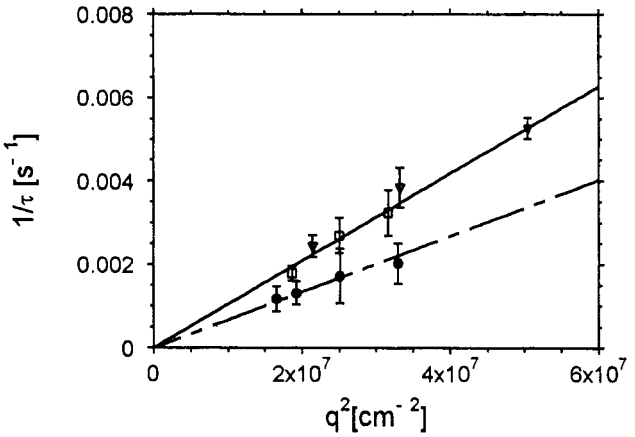

Figure 4. Inverse of decay times ($1/\tau$) as a function of q^2 for HSA adsorbed on PAH- and PSS-terminating films. The slope of the lines corresponds to diffusion coefficients $D = 1.0 \times 10^{-10}$ cm^2/s for the PAH (solid line)- and $D = 6.6 \times 10^{-11}$ cm^2/s for the PSS (dashed line)-terminating films. ●, HSA on PEI(PSS/PAH)$_2$PSS multilayer film; ▼, □, HSA on PEI(PSS/PAH)$_3$ multilayer film.

describe accurately the evolution of the signal only during an initial period. (See inset of Figure 3D.) This again shows the existence of a second more slowly diffusing protein population embedded between PSS layers. Surprisingly, as far as the diffusion coefficient is concerned, it seems higher for HSA molecules embedded between PSS layers in comparison with HSA adsorbed on PSS-terminating films (1.1×10^{-10} cm^2/s compared with 6.6×10^{-11} cm^2/s). On the other hand, no significant change of D is observed for HSA embedded between PAH layers when compared with HSA adsorbed on a PAH-terminating multilayer, both values being approximately 10^{-10} cm^2/s. One can notice that D values are similar for HSA in contact with PAH layers and HSA embedded between PSS layers.

The higher diffusivity of HSA deposited on PAH (polycation)-terminating films than on PSS (polyanion)-terminating ones, the increased diffusivity of HSA embedded between PSS layers when compared with HSA adsorbed on PSS-terminating films, and the existence of at least two populations of deposited proteins, "rapidly" diffusing ones and "slowly" or immobile proteins, are rather surprising results that must originate from the interplay of different interactions. The HSA molecules interact with the polyelectrolytes of the films, these polyelectrolytes interact themselves with the films, and finally, the HSA molecules can also interact one with each other. It is thus difficult to conclude from these experimental data about the precise contribution to the diffusion behavior of the proteins adsorbed on or embedded in the polyelectrolyte multilayers. The protein diffusion originally came from the direct mobility of the proteins with respect to the multilayer films and/or also from the diffusion of the polyelectrolytes interacting with the proteins along the film. Unfortunately, to our knowledge, no study of the mobility of the polyelectrolytes in a multilayer film exist up to now. The existence of at least two protein populations on the surface can originate from the fact that proteins may interact in different ways with the polyelectrolytes. The immobile or slowly diffusing HSA molecules might be strongly bound to polyelectrolytes that are highly entangled in the neighboring polyelectrolyte layers as suggested by the interdigitation of adjacent layers[17,18] whereas the rapidly diffusing ones could be bound to less entangled polyelectrolytes. This would also require the existence of rapidly diffusing and slowly or immobile polyelectrolytes in the multilayer. Another reason could be the fact that protein molecules at high concentrations have the tendency to aggregate by forming intermolecular β-sheet structures.[27] Such aggregates are expected to diffuse much more slowly along the surface than single albumin molecules. With PSS interacting less strongly with HSA than PAH at pH 7.4, it is expected that the tendency to form HSA aggregates is stronger on PSS- than on PAH-terminating films. This leads to a smaller diffusion coefficient of HSA on PSS- than on PAH-terminating films, as it was observed experimentally. The fact that the D increases when HSA is embedded between PSS layers when compared with HSA adsorbed on a PSS-terminating film may also be because embedding of proteins prevents protein aggregation as it is observed for fibrinogen embedded in PSS/PAH multilayers.[27] This effect should be less pronounced on PAH, which already interacts strongly with HSA when it is adsorbed on a PAH-terminating film. Additional studies are needed to understand the physical origin of these protein behaviors in multilayers films. In particular, it would be of interest to try to correlate such diffusion experiments with the structural evolution of the proteins on and in these films. One should also investigate the diffusion properties of the polyelectrolytes constituting the films in these architectures.

Conclusion

We present the first results relative to the diffusion process of proteins (HSA) adsorbed on or embedded in PSS/PAH polyelectrolyte multilayer films. Our experiments show the existence of at least two populations of adsorbed proteins on the surface or in the multilayers. One population, which represents on the order of 50% of the adsorbed proteins, corresponds to proteins that are able to diffuse laterally along the surface or in the multilayers, whereas the others diffuse more slowly or seem almost immobile over the experimental time scale. This constitutes a key result for the practical use of these systems as targeted biomaterial coatings, the ligand−receptor cell interactions requiring the clustering of the receptors on the cell membrane. Surprisingly, the diffusion coefficients of the mobile proteins adsorbed on or embedded in the polyelectrolyte multilayers seem to be of the same order of magnitude and are 1 order of magnitude smaller than on rigid substrates such as silica or PMMA. The values of the diffusion coefficients lie between 10^{-10} and 10^{-11} cm^2/s.

Acknowledgment. This work was supported by the program "Adhésion Cellules-Matériaux" and by the program CNRS "Physique et Chimie du Vivant". It was performed within the framework of the CNRS/INSERM Research Network "Mécanismes physico-chimiques d'adhésion cellulaire: forces d'adhésion entre ligands et récepteurs biologiques."

LA0104469

(27) Schwinte, P.; Voegel, J.-C.; Picart, C.; Haikel, Y.; Schaaf, P.; Szalontai, B., accepted in *J. Phys. Chem.*.